Symbiosis

www.symbiosisonline.org
www.symbiosisonlinepublishing.com
ISSN Online: 2374-8141

Research article | Nanoscience & Technology: Open Access | Open Access

Analytical Solutions to the Problem of the Grain Groove Profile

Tayssir Hamieh[1,2*], Zoubir Khatir[1] and Ali Ibrahim[1]

[1]Systèmes et Applications des Technologies de l'information et de l'Energie (SATIE), Institut français des sciences et technologies des transports, de l'aménagement et des réseaux (IFSTTAR), 25 Allée des Marronniers, 78000, Versailles, France

[2]Laboratory of Materials, Catalysis, Environment and Analytical Methods (MCEMA) and LEADDER Laboratory, Faculty of Sciences and EDST, Lebanese University, Hariri Campus, Hadath, Beirut, Lebanon

Received: June 29, 2018; Accepted: July 17, 2018; Published: August 1, 2018

***Corresponding author:** Tayssir Hamieh, SATIE, IFSTTAR, 25 Allée des Marroniers, 78000, Versailles, France and MCEMA, LEADDER, Faculty of Sciences and EDST, Lebanese University, Beirut, Lebanon, E-mail : tayssir.hamieh@ul.edu.lb ; zoubir.khater@ifsttar.fr*

Abstract

During the last sixty years, the problem of the formation of grain boundary grooving in polycrystalline thin films, was largely studied, analyzed and commented. The thermal effect on the properties of the grain boundary grooving was first studied by Mullins in his famous paper published in 1957 and then by other authors. This paper constitutes a new contribution on the correction of Mullins problem in the case of the evaporation-condensation and proposes a more accurate solution of the partial differential equation governing the geometric profile of the grain boundary grooving. The Mullins hypothesis neglecting the first derivative ($|y'| \ll 1$) in the main equation was defeated by our new solution. In this paper, we proved that the new proposed mathematical solution giving the solution $y(x, t)$ is valid for all x values without any approximation on the first derivative y'.

Introduction

The study of grain boundary grooves at the surface of polycrystalline thin films is of vital importance, and especially in nanomaterial sciences applied to electric and electronic processes. Many studies on thin polycrystalline films showed that when these films are submitted to a sufficient thermal treatment, several holes can be formed conducting to the degradation of materials [1-9]. The failure of the films resulted from the formation of grain boundary grooves [9].

The thermal grooving along grain boundaries is certainly responsible for the failure initiation produced in the films at the intersection of grain boundaries. The grain boundary grooving is an important factor in two dimensional grain growth of thin films [10]. The deepening of grain boundary grooves at the surface tends to pin the boundaries and impede grain growth, ultimately causing stagnation of the evolution [10-13]. The morphological profile of the sloping sides is important because the local slope determines the driving force for grain growth required for the boundary to break free of the groove [10]. Mullins studied the thermal grooving, with an isotropic surface free energy, by either surface diffusion or evaporation–condensation processes [11].

It was observed that the first phase of aging is classically associated with the reconstruction of the metallization and the degradation of the bonding contact. The end of life is rather characterized by bond-wire heel-cracks and lift-off [14].

During the last sixty years, the problem of the thermal degradation and the formation of grain boundary grooving in polycrystalline thin films, was largely studied, analyzed and commented [15-24]. The thermal effect on the properties of the grain boundary grooving was first studied by Mullins in his famous paper published in 1957 and then by many other authors [15,18-24].

Chen proposed a stochastic theory of normal grain growth. His model was based on the concept that the migration of kinks and ledges should cause a Brownian motion of the grain boundary [25]. Chen proved that this motion results in a drift of the grain size distribution to larger sizes, and the kinetics of grain growth is related to the kinetics of kinks and ledges; specifically, via the rates of nucleation, recombination and sink annihilation [25].

Agrawal, R. Rajhave found that thin films of polycrystalline zirconia, deposited on a sapphire substrate become gradually discontinuous when annealed at high temperature [26]. They identified the nucleation and growth mechanism of cavities where zirconia grain boundaries meet the substrate, and proved a dependency of cavity nucleation and orientation on the interfacial energies.

The kinetics of cathode edge shrinkage and displacement coupled strongly with the grain boundary grooving was investigated by Ogurtani and Akyildiz using the novel mathematical model developed by Ogurtani in sandwich type thin film bamboo lines [26,27,28].

The study of grain boundary grooves is important in material processing and synthesis. When a vertical grain boundary ends at a horizontal free surface, a groove forms at the tip to reduce the combined grain-boundary and surface energies. Min and

Wong studied the grain-boundary grooving by capillarity-driven surface diffusion with asymmetric and strongly anisotropic surface energies [29].

There is an important effect of the thermal treatment on the degradation of metallized films, and especially, on the metallization used in electronic components. Power electronic modules are key elements in the chain of power conversion. The application areas include aerospace, aviation, railway, electrical distribution, automotive, home automation, oil industry. These modules constitute an assembly of various materials (Figure 1). Generally, the power chips are carried on a ceramic substrate that must ensure good electrical insulation and good thermal conduction. This substrate is also welded on a sole to be cooled.

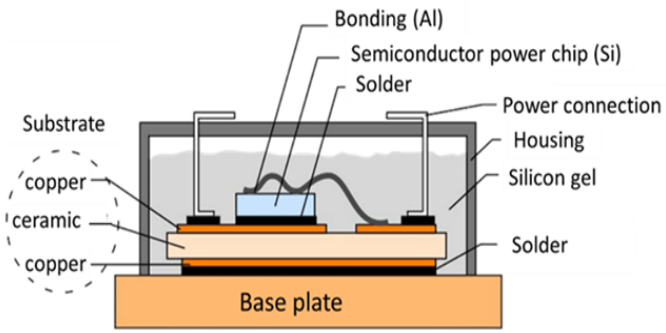

Figure 1: High power IGBT module

The assembly technologies are various. This includes materials and process for insulation or passivation, interconnections, and die attach. The topside interconnections in power semiconductor devices, consisting of the metallization and the wire bonds, are subjected in operation to high functional stresses. This is the result of an important difference between the coefficients of thermal expansion (CTE) of the materials in contact: metallization and wire bonds (aluminum) and dies (silicon). The metallization layer (around 5 µm) deposited on the chips becomes a lot more distorted than the silicon with temperature, leading to high tensile and compressive stresses and thus to large inelastic strains [30]. It has been reported that two main types of degradation can take place in the topside of power chips under the effect of thermo mechanical cycles: metallization reconstruction and degradation of bonding contacts (Figure 2 and 3) [30-32]. The last one may itself be either heel-cracks or cracks propagation followed by lift-off [33]. Various works have been conducted to propose scenarios of degradation mechanisms using thermal and power cycling tests [34-36]. Although it is quite clear that the wire-bond lift-off contributes mainly to the module failure [37], this link is not obvious with the metallization degradation [35].

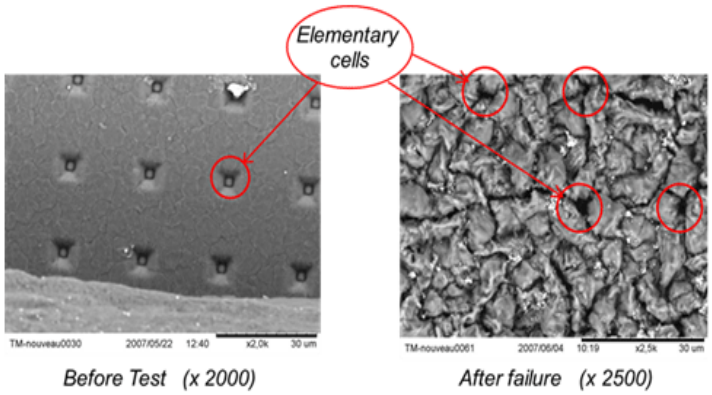

Figure 2: Topside metallization: before and after aging

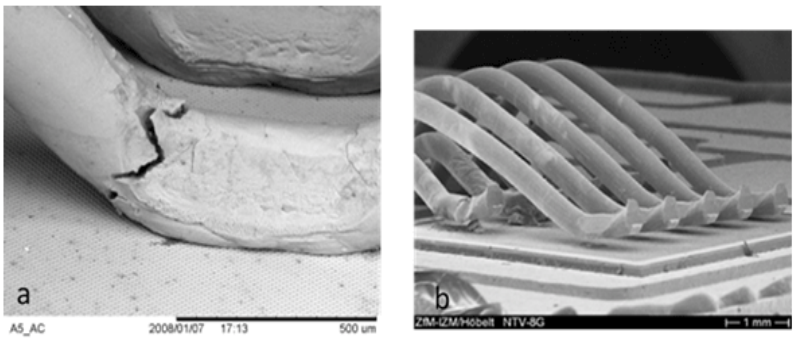

Figure 3: a) Heel cracks, **b)** Lift off

Mullins developed the two cases of the evaporation-condensation and the surface diffusion by formulating in both cases the mathematical problem of the partial differential equation governing the geometric profile of the grain boundary grooving [15-17].

The method consisted in using the general relation of the curvature R at any point (x, t) of the profile, where y = y(x, t) and R is a function of the two first derivatives y' and y" as a function of x. All mathematical developments proposed by Mullins [15, 16], Mullins and al. and many other researchers were based on the approximation given by $|y'| \ll 1$ [11,20,22-24].

This paper is a contribution to a better understanding of the effects of stress parameters on the degradation mechanisms of the top side interconnections. In this paper, we reconsidered the Mullins problem by considering the problem of the evaporation-condensation proposing a new mathematical solution and obtaining an analytical solution giving the solution y (x, t) taking into account the boundary conditions independently of any conditions of y'(x).

Formulation of the Problem

It was observed that a two dimensional metallic film remains flat for any temperatures and for a very long time. When the temperature increases, the metal atoms move causing grooves at the grain boundary surface. The metallic atoms can diffuse at the surface or in the volume. Atoms can also evaporate into the vapor phase or condensate. Mullins developed the grooving process produced in solid surfaces [11]. Grain-boundary migration controls the growth and shrinkage of crystalline grains and is important in materials synthesis and processing. A grain boundary ending at a free surface forms a groove at the tip, which affects its migration [18]. In polycrystalline thin films, grain boundary grooving through the thickness of the film is a common failure mode that strongly affects their properties. The grooving forms and develops at the point of intersection when the grain boundary ends at a free boundary in order to reduce the total free energy [10]. As example, we give on Figure 4 the symmetric profile of grain boundary grooving of a thin film.

It was experimentally shown that when thin polycrystalline films are annealed, they tend to break up by the formation

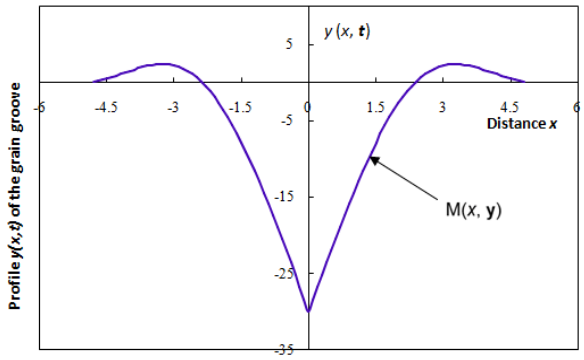

Figure 4: Profile y(x,t) of the grain boundary groove.

and growth of grooves [7, 8, 38-45]. Smaller and larger holes are usually located at the intersection points of three-grain boundaries [9]. The break up in thin films of some metals as copper on sapphire was initiated at processing defects in the film ,in contrast of cavities found at grain boundaries on zirconia on alumina polycrystalline films [7,26].

Galina and Fradkov studied the problem of the grain boundary hole development by assuming that there is evaporation/condensation as the transport mechanism rather than surface diffusion as generally supposed [46,47]. Mullins studied the thermal grooving mechanisms relative to the evaporation/condensation and surface diffusion phenomena [15]. Mullins supposed for a polycrystalline solid at equilibrium, a symmetric grain boundary groove profile and then the ratio of grain boundary energy per unit area, γ_{GB}, to surface energy per unit area, γ_{SV}, is related to the groove angle, ⍰ by this relationship:

$$\frac{\gamma_{GB}}{2\gamma_{SV}} = Sin\theta$$

Note that tanθ is equal to the slope of the profile y(x,t) at x = 0.

When studying the evolution of grain boundary groove profiles in the cases of the evaporation/condensation and surface diffusion, Mullins assumed that: (1) the surface diffusivity and the

surface energy, γ_SV, were independent of the crystallographic orientation of the adjacent grains and (2) the tangent of the groove root angle, θ, is small compared to unity [15]. Mullins also supposed an isotropic material. The assumption (tanθ << 1) was used in all papers' Mullins to simplify the study of the mathematical partial differential equation. The polycrystalline metal was supposed (3) in quasi-equilibrium with its vapor. The interface properties doesn't depend on the orientation relative to the adjacent crystals. The grooving process was described by Mullins using the macroscopic concepts (4) of surface curvature and surface free energy. The matter flow (5) is neglected out of the grain surface boundary.

We propose in this paper to study the grain boundary groove profiles in polycrystalline metal and to give an analytical solution relative to the only case of evaporation/ condensation, more precise than of the solution found by Mullins that supposed very small slops for all x values [15].

On Figure 4, we give the profile y(x,t) of the grain boundary groove in metal polycrystal.

By using the notion of curvature c at any point M(x; y(x, t)) given by the following relation:

$$c = \frac{1}{R} = -\frac{y''(x)}{\left[1+y(x)^2\right]^{\frac{3}{2}}} \quad (1)$$

Where R is the curvature radius at point M

$$y'(x) = \frac{\partial y}{\partial x} \quad \text{and} \quad y''(x) = \frac{\partial^2 y}{\partial x^2}$$

The mathematical equation governing the evaporation-condensation problem can be written here as:

$$\frac{\partial y}{\partial t} = C(T)\frac{y''(x)}{\left(1+y(x)^2\right)} \quad (2)$$

Where C(T) a constant of the problem depending on the temperature T, given by:

$$C(T) = \mu\frac{P_0(T)\gamma(T)\omega^2}{\sqrt{2\pi mkT}} \quad (3)$$

where γ is the isotropic surface energy, $P_0(T)$ the vapor pressure at temperature *T* in equilibrium with the plane surface of the metal characterized by a curvature *c* = 0, ω is the atomic volume, *m* is molecular mass, μ the coefficient of evaporation and k is the Boltzmann constant.

Mullins [10] supposed that the coefficient of evaporation μ is equal to the unit.

Mullins Approximation

To resolve this differential equation, Mullins was constraint to suppose that |y'|≪1 that means that the slope y'(x,t) at any point of the curve y (x, t) is very small behind 1 and can be neglected. Equation (4) can be written as:

$$\frac{\partial y}{\partial t} = C(T)y''(x) \quad (4)$$

With the boundary conditions:

$$\begin{cases} y(x,0) = 0 \\ y'(0,t) = \tan\theta = m \end{cases} \quad (5)$$

This problem is well-known in the conduction of heat in solids. It can be resolved by the following variable change:

$$u = \frac{x}{2\sqrt{Ct}} \quad (6)$$

and one obtains the derivatives of u as a function of x and t:

$$\begin{cases} \frac{\partial u}{\partial x} = \frac{u}{x} \\ \frac{\partial u}{\partial t} = -2C\frac{u^3}{x^2} \end{cases} \quad (7)$$

Now, using $\frac{\partial y}{\partial t} = \frac{\partial y}{\partial u}\frac{\partial u}{\partial t}$ and $\frac{\partial y}{\partial x} = \frac{\partial y}{\partial u}\frac{\partial u}{\partial x}$ one obtains the following derivatives:

$$\frac{\partial y}{\partial t} = -2C\frac{u^3}{x^2}\frac{\partial y}{\partial u} \quad (8)$$

$$y'(x) = \frac{\partial y}{\partial x} = \frac{u}{x}\frac{\partial y}{\partial u} \quad (9)$$

$$y''(x) = \frac{\partial^2 y}{\partial x^2} = \left(\frac{u}{x}\right)^2\frac{\partial^2 y}{\partial u^2} \quad (10)$$

Then, equation (4) becomes as a function of u:

$$\frac{\partial^2 y}{\partial u^2} = -2u\frac{\partial y}{\partial u} \quad (11)$$

and

$$\frac{y''(u)}{y'(u)} = -2u \quad (12)$$

The solution of differential equation (12) is given by:

$$y'(u) = Ae^{-u^2}$$

With A a constant of the problem.

Knowing that $\frac{\partial y}{\partial u} = \frac{\partial y}{\partial x}\frac{\partial x}{\partial u}$, we obtain:

$$\frac{\partial y}{\partial u} = 2\sqrt{Ct}\frac{\partial y}{\partial x} \quad (13)$$

With the condition boundary y'(0,t) =m, one obtains $A = 2m\sqrt{Ct}$. Using the other condition boundary y (x, 0) = 0, the solution of the differential equation (13) becomes:

$$y = 2m\sqrt{Ct}\int_0^u e^{-u^2}du + Cst, \quad u = \frac{x}{2\sqrt{Ct}} \quad (14)$$

The constant Cst can be determined by the boundary condition y(∞,t)=0. This gives:

$$2m\sqrt{Ct}\int_0^{\infty} e^{-u^2}\,du + Cst = 0 \quad (15)$$

With $\int_0^{\infty} e^{-u^2}\,du = \frac{\sqrt{\pi}}{2}$ one obtains: $Cst = -2m\sqrt{Ct}\frac{\sqrt{\pi}}{2}$ and equation (15) can be written:

$$y = 2m\sqrt{Ct}\int_0^{\frac{x}{2\sqrt{Ct}}} e^{-u^2}\,du - 2m\sqrt{Ct}\frac{\sqrt{\pi}}{2} = -m\sqrt{\pi Ct}\left[1 - \frac{2}{\sqrt{\pi}}\int_0^{\frac{x}{2\sqrt{Ct}}} e^{-u^2}\,du\right]$$

In conclusion, the solution of approximated Mullins problem will be written as:

$$y(x,t) = -m\sqrt{\pi Ct}\left[1 - \frac{2}{\sqrt{\pi}}\int_0^{\frac{x}{2\sqrt{Ct}}} e^{-u^2}\,du\right] \quad (16)$$

In conclusion for this part, the Mullins solution of approximated equation supposing $|y'| \ll 1$, is given by:

$$\begin{cases} y(x,t) = -m\sqrt{\pi Ct}\,erfc\left(\frac{x}{2\sqrt{Ct}}\right) \\ y'(u) = 2m\sqrt{Ct}e^{-u^2}, \text{with} u = \frac{x}{2\sqrt{Ct}} \end{cases} \quad (17)$$

Where erfc is the complementary error function.

However, knowing that $(0,t) = -\varepsilon_0$, one deduces the value of the groove depth:

$$\varepsilon_0(t) = m\sqrt{\pi Ct} = tan\theta\sqrt{\pi Ct} \quad (18)$$

The obtained calculations are presented on Figure 5 showing the variation of the profile y(x, t) of the grain groove of Mullins approximation as a function of the distance x from the grain separation surface for various angles θ. It is obvious shown that when the groove angle θ increases, the slope m at x = 0 increases and this increases the groove depth ε_0 as proved by Figure 5. However, all representative curves obtained in this case are located under the x-axis meaning that y(x,t) is negative for all x values without any inflexion point. There is no maximum for these curves. This means that the Mullins solution cannot describe correctly the experimental observations shown in Figure 4.

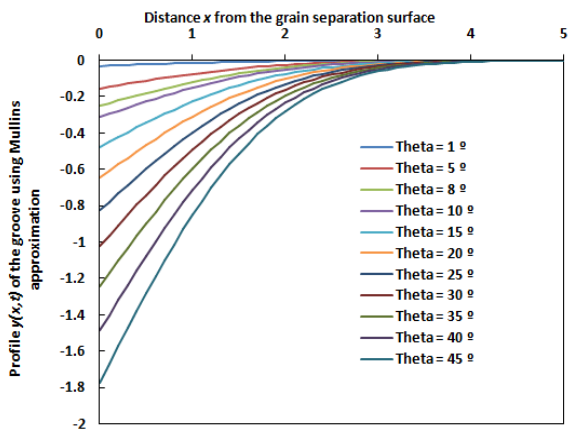

Figure 5: Evolution of the profile y(x, t) of the grain groove of Mullins approximation as a function of the distance x from the grain separation surface for various groove angles θ from 1º to 45º.

On Figure 6, we plotted the variations of the derivative y'(x) of the grain groove profile for Mullins approximation as a function of the distance x from the grain separation surface for various angles θ. This derivative strongly depends on the groove angle. The smaller the groove angle is, the smaller the derivative y' is. For θ. = 1°, all derivatives $y^1(x)$ can be neglected relatively to 1 for all x values. In this nonrealistic case and only in this case, the Mullins approximation can be applied and the solution can describe the profile of the grain groove in the case of evaporation-condensation. However, Figure 6 shows that the Mullins derivatives for all groove angles are positive implying the non-existence of a maximum of groove profile that can be observed in the experiments.

It is clearly shown on Figure 6 that for a groove angle and greater than 5°, all derivative values y' (x) are greater than 0.25 whatever the x value and become greater than 1 when θ > 25°. In all cases, the Mullins approximation cannot be applied when the groove angle θ > 5° and the Mullins condition |y'|≪1 becomes invalid in such cases.

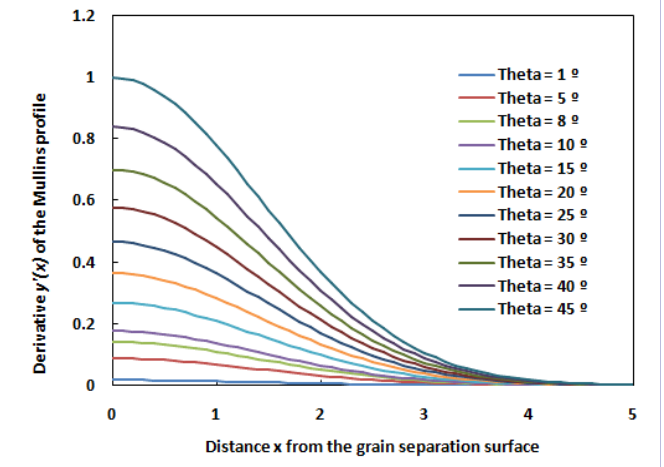

Figure 6: Evolution of the derivative y' (x) of the grain groove profile of Mullins approximation as a function of the distance x from the grain separation surface for various groove angles θ.

It is clearly shown on Figure 6 that for a groove angle and greater than 5°, all derivative values y' (x) are greater than 0.25 whatever the x value and become greater than 1 when θ >25°. In all cases, the Mullins approximation cannot be applied when the groove angle θ > 5° and the Mullins condition |y'|≪1 becomes invalid in such cases.

In order to more clarify the non-validity of the Mullins hypothesis in general, we give below on Table 1 the error

Table 1: Evaluation of the errors (in %) made when supposing $|y'| << 1$, for different groove angle values

x	θ = 1º	θ = 5º	θ = 10º	θ = 20º	θ = 30º	θ = 40º	θ= 45º
0	1.7	8.7	17.6	36.4	57.7	83.9	100
0.1	1.7	8.7	17.6	36.3	57.6	83.7	99.8
0.2	1.7	8.7	17.5	36	57.2	83.1	99
0.3	1.7	8.6	17.2	35.6	56.5	82	97.8
0.4	1.7	8.4	16.9	35	55.5	80.6	96.1
0.5	1.6	8.2	16.6	34.2	54.2	78.8	93.9
0.6	1.6	8	16.1	33.3	52.8	76.7	91.4
0.7	1.5	7.7	15.6	32.2	51.1	74.2	88.5
0.8	1.5	7.5	15	31	49.2	71.5	85.2
0.9	1.4	7.1	14.4	29.7	47.2	68.5	81.7
1	1.4	6.8	13.7	28.3	45	65.3	77.9
1.1	1.3	6.5	13	26.9	42.7	62	73.9
1.2	1.2	6.1	12.3	25.4	40.3	58.5	69.8
1.3	1.1	5.7	11.6	23.9	37.8	55	65.5
1.4	1.1	5.4	10.8	22.3	35.4	51.4	61.3
1.5	1	5	10	20.7	32.9	47.8	57
1.6	0.9	4.6	9.3	19.2	30.4	44.2	52.7
1.7	0.8	4.2	8.6	17.7	28	40.7	48.6
1.8	0.8	3.9	7.8	16.2	25.7	37.3	44.5
1.9	0.7	3.5	7.2	14.8	23.4	34	40.6
2	0.6	3.2	6.5	13.4	21.2	30.9	36.8

percentages made when supposing |Y′|<<1, for different groove angle values. Table 1 clearly shows that the error percentage is higher than 10% from a groove angle θ exceeding 6°; the error dramatically increases to 17% for θ= 10° and exceeds 100% since θ = 45°. This proves that the Mullins approximation cannot be justified after θ = 6° and all results of the literature based on the condition |Y′|<< 1 are experimentally false.

These results lead us to reconsider the evaporation-condensation problem by proposing a new method taking into account the general equation without neglecting the first derivative y'(x). The new method consisting in the correction of Mullins solution is presented in the following section.

New Method for the Correction of Mullins Solution

We recall below the general equation of the evaporation-condensation problem:

$$\frac{\partial y}{\partial t} = C(T)\frac{y''(x)}{\left(1+y'(x)^2\right)}$$

Using the same notations given above, one writes:

$$\begin{cases} 1+y'(x)^2 = 1+\left(\dfrac{1}{2\sqrt{Ct}}\dfrac{\partial y}{\partial u}\right)^2 \\ \dfrac{\partial y}{\partial t} = -2C\dfrac{u^3}{x^2}\dfrac{\partial y}{\partial u} \\ y''(x) = \dfrac{\partial^2 y}{\partial x^2} = \left(\dfrac{u}{x}\right)^2\dfrac{\partial^2 y}{\partial u^2} \end{cases} \quad (19)$$

The three combined equations (19) then give:

$$-2C\frac{u^3}{x^2}\frac{\partial y}{\partial u} = C\frac{\left(\dfrac{u}{x}\right)^2\dfrac{\partial^2 y}{\partial u^2}}{1+\left(\dfrac{1}{2\sqrt{Ct}}\dfrac{\partial y}{\partial u}\right)^2} \quad (20)$$

The second order differential equation is then given by the expression (21):

$$y''(u) = -2uy'(u)\left(1+\frac{1}{4Ct}y'(u)^2\right) \quad (21)$$

In this paper, we propose a new method of resolution of equation (21) using the approximated Mullins solution: $y'(u) = 2m\sqrt{Ct}e^{-u^2}$ and replacing it in equation (21), one obtains

$$y''(u) = -4m\sqrt{Ct}ue^{-u^2}\left(1 + m^2e^{-2u^2}\right) \quad (22)$$

The first integration of equation (22) as a function of the variable *u* gives:

$$y'(u) = \frac{2}{3}m\sqrt{Ct}\left(3e^{-u^2} + m^2e^{-3u^2}\right) + Cst$$

Using the initial condition: y'(0) =2m√Ct, one obtains the constant value *C*st:

$$Cst = -\frac{2}{3}m^3\sqrt{Ct}$$

and equation (22) becomes:

$$y'(u) = \frac{2}{3}m\sqrt{Ct}\left(3e^{-u^2} + m^2e^{-3u^2}\right) - \frac{2}{3}m^3\sqrt{Ct} \quad (23)$$

As a function of x and t, we will obtain:

$$y'(x,t) = \frac{m}{3}\left(3e^{-\frac{x^2}{4Ct}} + m^2e^{-\frac{3x^2}{4Ct}}\right) - \frac{m^3}{3}$$

The second integration of equation (23) leads to:

$$y(u) = \frac{2}{3}m\sqrt{Ct}\left(3\int_0^u e^{-u^2}du + m^2\int_0^u e^{-3u^2}du\right) - \frac{2}{3}m^3\sqrt{Ct}u + y(0) \quad (24)$$

Equation (24) represents the new solution of the general problem given by equation (21)

Using the boundary condition $y(u_l)$=0, for u=u_l corresponding to x_l=2√Ct u_l, one obtains the following equation:

$$0 = \frac{2}{3}m\sqrt{Ct}\left(3\int_0^{u_l} e^{-u^2}du + m^2\int_0^{u_l} e^{-3u^2}du\right) - \frac{2}{3}m^3\sqrt{Ct}u_l + y(0)$$

Therefore, the equation (25) is obtained:

$$y(0) = -h_0 = \frac{2}{3}m^3\sqrt{Ct}u_l - \frac{2}{3}m\sqrt{Ct}\left(3\int_0^{u_l} e^{-u^2}du + m^2\int_0^{u_l} e^{-3u^2}du\right) \quad (25)$$

Where h_0 is the groove deep.

Equation (25) shows that the groove deep h_0 strongly depend on the time t, the grain length u_l, the constant C and the slope m at x = 0 and then on the groove angle θ .

If one uses the complementary error function erfc:

$$\int_0^X e^{-u^2}du = \frac{\sqrt{\pi}}{2}\left[1 - erfc(X)\right],$$

$$\int_0^X e^{-3u^2}du = \frac{\sqrt{\pi}}{2\sqrt{3}}\left[1 - erfc\left(\sqrt{3}X\right)\right]$$

with $X = \frac{x}{2\sqrt{Ct}}$, equations (24) and (25) can be written as:

$$\begin{cases} y(u) = \frac{2}{3}m\sqrt{Ct}\left[\frac{3\sqrt{\pi}}{2}\left[1 - erfc(u)\right] + \frac{\sqrt{\pi}}{2\sqrt{3}}m^2\left[1 - erfc\left(\sqrt{3}u\right)\right]\right] - \frac{2}{3}m^3\sqrt{Ct}u + y(0) \\ y(0) = -h_0 = \frac{2}{3}m^3\sqrt{Ct}u_l - \frac{2}{3}m\sqrt{Ct}\left[\frac{3\sqrt{\pi}}{2}\left[1 - erfc(u_l)\right] + \frac{\sqrt{\pi}}{2\sqrt{3}}m^2\left[1 - erfc\left(\sqrt{3}u_l\right)\right]\right] \end{cases}$$

As a function of (x,t), one obtains:

$$\begin{cases} y(x,t) = -m\sqrt{\pi Ct}erfc\left(\frac{x}{2\sqrt{Ct}}\right) + \frac{m^3}{3}\sqrt{\frac{\pi Ct}{3}}\left[1 - erfc\left(\sqrt{\frac{3}{Ct}}\frac{x}{2}\right)\right] - \frac{m^3}{3}x + m\sqrt{\pi Ct} + y(0) \\ y(0,t) + m\sqrt{\pi Ct} = \frac{m^3}{3}x_l + m\sqrt{\pi Ct}erfc\left(\frac{x_l}{2\sqrt{Ct}}\right) - \frac{m^3}{3}\sqrt{\frac{\pi Ct}{3}}\left[1 - erfc\left(\sqrt{\frac{3}{Ct}}\frac{x_l}{2}\right)\right] \end{cases} \quad (26)$$

Taking into account the Mullins solution, one can write the new solution as:

$$y(x,t) = y_{Mullins}(x,t) + \frac{m^3}{3}\sqrt{\frac{\pi Ct}{3}}\left[1 - erfc\left(\sqrt{\frac{3}{Ct}}\frac{x}{2}\right)\right] - \frac{m^3}{3}x + m\sqrt{\pi Ct} + y(0) \quad (27)$$

Equation (27) obviously shows the large difference between the Mullins solution and the proposed solution.

On Figure 7, we draw the variations of the profile y(x, t) of the grain groove of the new solution as a function of the distance x from the grain separation surface for various angles θ. Two cases can be distinguished here:

The first one is relative to small angles θ from 1° to 15° (Figure 7 a), where we can see an identical curve with that of Mullins solution with a difference for the groove deep value. There is an over estimation in the values obtained by Mullins. The difference between our solution and Mullins solution can reach 20% for the groove deep in this case.

The second case concerns larger angles θ from 20° to 45° (Figure 7 b). Here, it can be observed an important difference between the classical and new solutions. The new solution can easily explain the physical presence of a maximum of y for a certain value of x. whereas, the curves obtained by Mullins are monotonous and do not present any change in the derivative . that is constantly positive whatever the x value.

On Figure 8, we give the evolution of the derivative *y' (x)* of the grain groove profile obtained by the new solution for various groove angles θ from 1° to 45° . Here, there is no restriction concerning the value of the first derivative of the grain groove profile. The new results given by our solution confirm the experimental results given in literature showing a maximum of groove profile and then a decrease after this maximum [7, 9, 10, 14, 22-25]. The new derivative clearly shows a change in the sign of the solution y and its cancellation and then the presence of a maximum.

Comparison between Mullins Solution and the New Solution

The following expression gives the ratio of Mullins solution $y_{Mullins}$ on the corrected solution $y_{corrected}$:

$$\frac{y_{Mullins}}{y_{corrected}} = \frac{y_{Mullins}(x,t)}{y_{Mullins}(x,t) + \frac{m^3}{3}\sqrt{\frac{\pi Ct}{3}}\left[1 - erfc\left(\sqrt{\frac{3}{Ct}}\frac{x}{2}\right)\right] - \frac{m^3}{3}x + m\sqrt{\pi Ct} + y(0)} \quad (28)$$

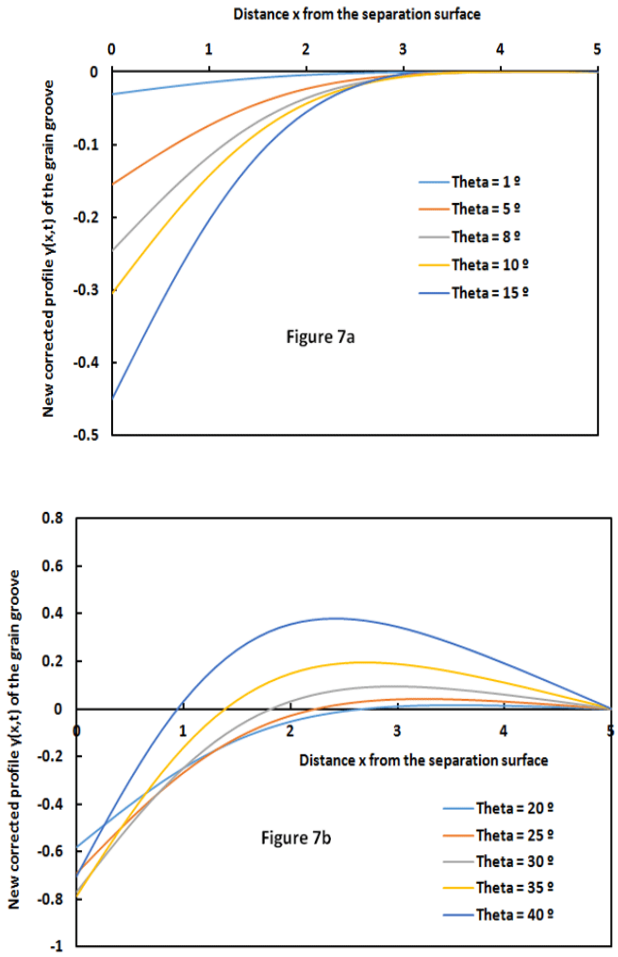

Figure 7a: Evolution of the profile y(x, t) of the grain groove of the new solution as a function of the distance x from the grain separation surface for various groove angles θ. Case of small angles θ from 1° to 15° (a) and larger angles θ from 20° to 45° (b).

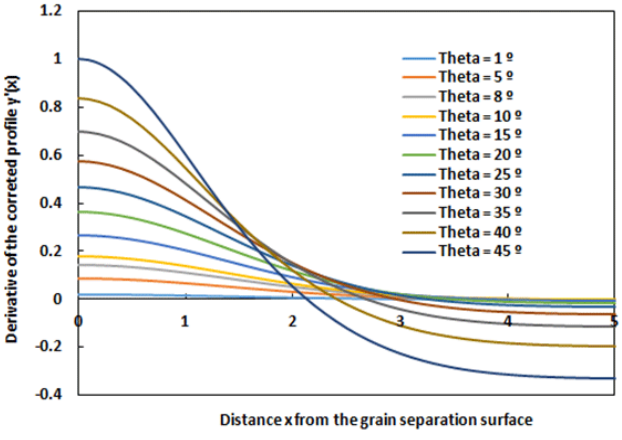

Figure 8: Evolution of the derivative y'(x) of the grain groove profile of the corrected solution as a function of the distance x from the grain separation surface for various groove angles θ.

On Figure 9, we represent the variations of the ratio ($y_{Mullins}/y_{corrected}$) as a function of the distance x from the grain separation surface for various groove angles θ. The only case that the two solutions are the same is that when the groove angle θ = 1°. For all other values of θ = 5°, the two solutions are different. The curves of Figure 9 prove that the Mullins solution is so far from the reality. There is an over estimation of y values given by Mullins solution. As example, we draw on Figure 10, the evolution of the profile y (x) of the grain groove for Mullins approximation and the new solution as a function of the distance x from the grain separation surface for θ = 35°. The two obtained curves show an important difference between the two cases.

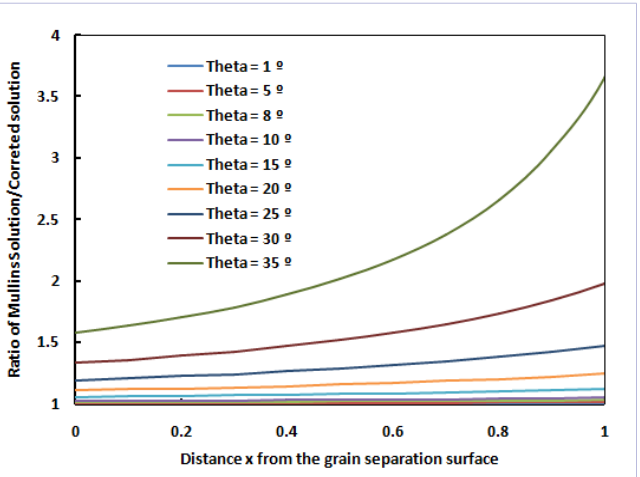

Figure 9: Evolution of the ratio ($y_{Mullins}$)/$y_{corrected}$) of Mullins solution on the corrected solution for the grain groove profile as a function of the distance x from the grain separation surface for various angles θ.

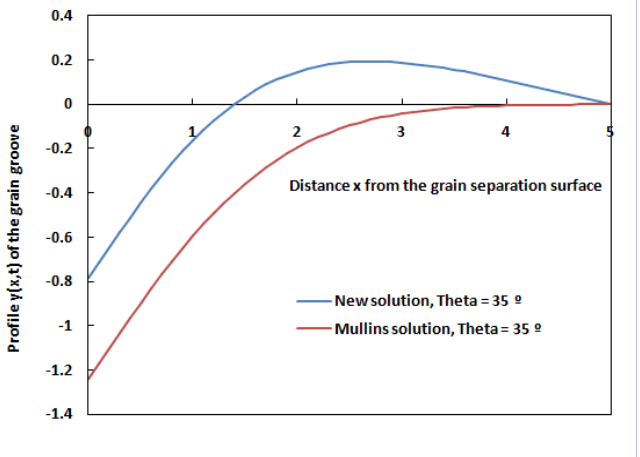

Figure 10: Evolution of the profile y (x) of the grain groove for Mullins approximation and the new solution as a function of the distance x from the grain separation surface for θ = 35°.

The ratio of the Mullins derivative $y'_{(Mullins)}$ and the corrected derivative $y'_{corrected}$ is given by the following expression:

$$\frac{y'_{Mullins}}{y'_{corrected}} = 1 + \frac{m^2}{3}\left(e^{-2u^2} - e^{+u^2}\right) \quad (29)$$

To compare between the two derivatives of Mullins and new solution, we draw on the Figure 11, the evolution of the derivative *y'(x)* of the grain groove profile for Mullins approximation and the new proposed solution as a function of the distance x from the grain separation surface for θ = 45°. The two obtained curves show an extreme deviation when the distance x increases.

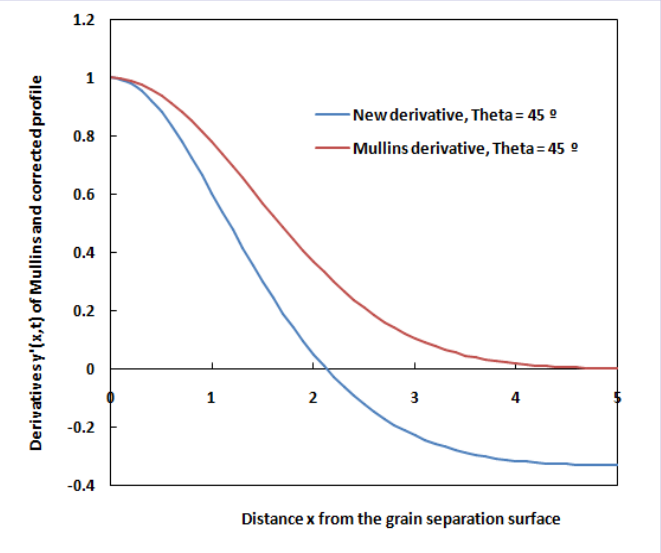

Figure 11: Evolution of the derivative y'(x) of the grain groove profile for Mullins approximation and the new proposed solution as a function of the distance x from the grain separation surface for θ = 45°

Conclusion

This original study proposed a mathematical correction to the Mullins problem of the grain boundary groove profile relative to the case of evaporation/condensation. We proved that the solution found by Mullins in his famous paper is false [10]. This validity of Mullins solution is only assured for non-realistic case of a groove angle $q \approx 1^{\circ}$ to 2°. The Mullins's hypothesis expressed by $|y'| << 1$ is is not satisfied. The obtained results proved that the error percentage of Mullins solution reaches 100% for values of the groove angle less than 45º. The Mullins solution over estimates the real values of the solution y of the groove profile.

The new found solution is given by the following equation:

$$y\ (x,t) = y_{Mullins}\ (x,t) + \frac{m^3}{3}\sqrt{\frac{\pi Ct}{3}}\left[1 - erfc\left(\sqrt{\frac{3}{Ct}}\frac{x}{2}\right)\right] - \frac{m^3}{3}x + m\sqrt{\pi Ct} - h_0$$

The result of the new solution is the confirmation of the experimental profile tendency justifying the presence of a maximum of distance x from the surface boundary. On the other hand, our solution was able to predict the groove deep h_0 by the following equation:

$$h_0 = +m\sqrt{\pi Ct} - \frac{m^3}{3}x_l - m\sqrt{\pi Ct}\,erfc\left(\frac{x_l}{2\sqrt{Ct}}\right) + \frac{m^3}{3}\sqrt{\frac{\pi Ct}{3}}\left[1 - erfc\left(\sqrt{\frac{3}{Ct}}\frac{x_l}{2}\right)\right]$$

It was proved that the groove deep strongly depend on the problem constant C, the time t, the slope of the profile at the origin or the groove angle θ and the grain length x_l.

As perspective, another study is preparing and concerns the general solution of the partial differential equation of the groove boundary profile, when combining the two cases relative to evaporation/condensation and surface diffusion.

References

1. ML Gimpl, AD Mc Master, N Fuschillo. Amorphous Oxide Layers on Gold and Nickel Films Observed by Electron Microscop. J. appl. Phys. 2004;35(12):3572-3575.
2. L Bachmann, DL Sawyer, BM Siegel. Observations on the Morphological Changes in Thin Copper Deposits during Annealing and Oxidation. J. appl. Phys. 2004;36(1):304.
3. Presland AEB, Price GL, Trimm DL, Kinetics of hillock and island formation during annealing of thin silver films. Prog. Surf. Sci. 1972;3:63-96. doi:10.1016/0079-6816(72)90006-8
4. Sharma SK, Spitz J. Hillock formation, hole growth and agglomeration in thin silver films. Thin Solid Films. 1980;65(3):339-350.
5. Wu NL, Philips J. Reaction-enhanced sintering of platinum thin films during ethylene oxidation. J. appl. Phys.1986;59(3):769-779.
6. Lee SY, Hummel RE, Dehoff R T. On the role of indium underlays in the prevention of thermal grooving in thin gold films. Thin Solid Films. 1987;149(1):29-48.
7. Kennefick CM,Raj R. Copper on sapphire: Stability of thin films at 0.7 Tm. Acta metall. 1989;37(11):2947-2952.
8. Miller KT, Lange FF, Marshall DB. The instability of polycrystalline thin films: Experiment and theory. J. Mater. Res. 1990;5(1):151-160.
9. Génin FY, Mullins WW, Wynblatt P. Capillary instabilities in thin films: A model of thermal pitting at grain boundary vertices. Acta Metallurgica et Materialia.1992;40 (12):3239-3248.
10. Stone HA, Aziz MJ, Margetis D. Grooving of a grain boundary by evaporation–condensation below the roughening transition. J. Appl. Phys. 2005;97(11):113535-113536.
11. Mullins WW. The effect of thermal grooving on grain boundary motion. Acta Metallurgica.1958;6(6):414-427.
12. Frost HJ, Thompson CV, Walton DT. Simulation of thin film grain structures—I. Grain growth stagnation. Acta. Metall. Mater. 1990; 38:1455-1462.
13. Lou C, Player M A. Advection-diffusion model for the stagnation of normal grain growth in thin films. J. Phys. D: Applied Physics. 2002;35:1805-1811.
14. Smet V, Forest F, Huselstein J, Rashed A, Richardeau F. Evaluation of Vce Monitoring as a Real-Time Method to Estimate Aging of Bond Wire-IGBT Modules Stressed by Power Cycling. IEEE Transactions on Industrial Electronics. 2013;60(7):2760-2770. doi: 10.1109/TIE.2012.2196894
15. Mullins WW. Theory of thermal grooving, Journal of Applied Physics. 1957;28(3):333-339.
16. Mullins WW. Grain boundary grooving by volume diffusion. Transactions of the Metallurgical Society of AIME. 1960;218:354-361.

17. Zhang H, Wong H. Coupled grooving and migration of inclined grain boundaries: regime I. Acta Materialia. 2002;50(8):1983–1994.
18. Bouville M, Dongzhi C, Srolovitz DJ. Grain-boundary grooving and agglomeration of alloy thin films with a slow diffusing species. Physical Review Letters. 2007;98(8).
19. Bouville M. Effect of grain shape on the agglomeration of polycrystalline thin films. Applied Physics Letters. 2007;90(6).
20. Genin FY, Mullins WW, Wynblatt P. The effect of stress on grain-boundary grooving. Acta Metall.1993;41:3541-3547.
21. Hackney SA. Grain-boundary grooving at finite grain size. Scripta Metall. 1988;22(11):1731-1735.
22. Klinger L, Glickman E, Fradkov V, Mullins W, Bauer C. Extension of thermal grooving for arbitrary grain-boundary flux. J. Appl. Phys. 1995;78:3833-3838.
23. Klinger L, Glickman E, Fradkov V, Mullins W, Bauer C. Effect of surface and grain-boundary diffusion on interconnect reliability, Mater. Res. Soc. Symp.Proc. 1995;391:295.
24. Brokman AKR, Mullins WW, Vilenkin AJ. Analysis of boundary motion in thin films, Scripta Metallurgica et Materialia. 1995;32(9);1341-1346.
25. I-W. Chen. A stochastic theory of grain growth. Acta Metallurgica. 1987;35(7):1723-1733.
26. Agrawal DC, Raj R. Autonucleation of cavities in thin ceramic films. Acta Metallurgica. 1989;37:2035-2038.
27. Ogurtani TO, Akyildiz O. Cathode edge displacement by voiding coupled with grain boundary grooving in bamboo like metallic interconnects by surface drift-diffusion under the capillary and electromigration forces. International Journal of Solids and Structures. 2008;45(3-4):921–942.
28. Ogurtani TO. Mesoscopic nonequilibrium thermodynamics of solid surfaces and interfaces with triple junction singularities under the capillary and electromigration forces in anisotropic three-dimensional space. Journal of Chemical Physics. 2006;124 (14): 144706-144712.
29. Ogurtani TO. Unified theory of linear instability of anisotropic surface and interfaces under capillary, electrostatic, and elastostatic forces: The growth of epitaxial amorphous silicon. Physical Review B. 2006;74: 155422–155447.
30. Min D, Wong H. Grain-boundary grooving by surface diffusion with asymmetric and strongly anisotropic surface energies, Journal of Applied Physics. 2006;99(2):023515 (2006).
31. M Ciappa. Selected failure mechanisms of modern power modules. Microelectr. Reliab.2002;42:653-667.
32. Detzel Th, Glavanovics M, Weber K. Analysis of wire bond and metallization degradation mechanisms in DMOS power transistors stressed under thermal overload conditions, Microelectr. Reliab. 2004;44:1485-1490.
33. Sebastiano Russo, Romeo Letor, Orazio Viscuso, Lucia Torrisi, Gianluigi Vitali. Fast thermal fatigue on top metal layer of power devices. Microelectr. Reliab. 2002;42:1617-1622.
34. Ramminger S, Seliger N, Wachutka G. Reliability Model for Al Wire Bonds subjected to Heel Crack Failures. Microelectron. Reliab. 2000;40(8-10):1521-1525.
35. Agyakwa PA, Yang L, Arjmand E, Evans P, Corfield MR, Johnson CM. Damage Evolution in Al Wire Bonds Subjected to a Junction Temperature Fluctuation on 30K. J. Electron. Mater. 2016;45(7):3659–3672.
36. Martineau D, Levade C, Legros M, Dupuy P, Mazeaud T. Universal Mechanisms of Al metallization ageing in power MOSFET devices. Microelectron. Reliab. 2014;54:2432-2439.
37. Pietranico S, Lefebvre S, Pommier S, Berkani Bouaroudj M, Bontemps S. A study of the effect of degradation of the aluminium metallization layer in the case of power semiconductor devices. Microelectron. Reliab. 2011;51(9-11):1824-1829.
38. Cova P, Fantini F. On the effect of power cycling stress on IGBT modules. Microelectron. Reliab. 1998;38(6-8):1347-1352.
39. Gimpl M L, Master A D Mc, Fuschillo N. Amorphous Oxide Layers on Gold and Nickel Films Observed by Electron Microscopy. J. appl. Phys. 2004;35(12):3572-3575.
40. Bachmann L, Sawyer D L and, Siegel B M. Observations on the Morphological Changes in Thin Copper Deposits during Annealing and Oxidation. J. appl. Phys. 2004;36(1):304-308.
41. Presland AEB,Price GL,Trimm DL.The role of microstructure and surface energy in hole growth and island formation in thin silver films. J. appl. Phys. 1972;29(2): 435-446.
42. Presland AEB,Price GL,Trimm DL. Kinetics of hillock and island formation during annealing of thin silver films. Prog. Surf. Sci.1972; 3(1):63-96.
43. Sharma SK, Spitz J. Hillock formation, hole growth and agglomeration in thin silver films. Thin Solid Films. 1980;65(3):339-350.
44. Hummel RE, Dehoff RT, Matts-Goho S, Goho WM, Thermal grooving, thermotransport and electrotransport in doped and undoped thin gold films. Thin Solid Films. 1981;78(1):1-14.
45. Wu NL, Philips J. Reaction-enhanced sintering of platinum thin films during ethylene oxidation. J. appl. Phys. 1998;59(3):769-779.
46. Palmer J E, Thompson CV, Smith HI. Grain growth and grain size distributions in thin germanium films. J. appl. Phys.1998;62(6): 2492-2497.
47. Galina AV, Fradkov V E, Shvindlerman LS. Rapid Penetration Along Grain Boundaries. Fiz. Khim. Mekh. Poverk.1988;1:105.